Materials Science and Engineering C 76 (2017) 1240–1247

Contents lists available at ScienceDirect

Materials Science and Engineering C

journal homepage: www.elsevier.com/locate/msec

Review

Electrochemical immunosensor based on ZnO nanorods-Au nanoparticles nanohybrids for ovarian cancer antigen CA-125 detection

Gisane Gasparotto [a,b], João Paulo C. Costa [b], Paulo I. Costa [c], Maria A. Zaghete [b], Talita Mazon [a,*]

[a] Center for Information Technology Renato Archer, CTI, Campinas, SP 13067-901, Brazil
[b] LIEC, Institute of Chemistry, São Paulo State University-UNESP, Araraquara, SP 14800-060, Brazil
[c] School of Pharmaceutical Sciences, São Paulo State University-UNESP, Araraquara, SP 14800-903, Brazil

ARTICLE INFO

Article history:
Received 20 September 2016
Received in revised form 30 November 2016
Accepted 7 February 2017
Available online 10 February 2017

Keywords:
Electrochemical immunosensor
ZnO
Nanohybrid materials
CA-125
Au nanoparticles

ABSTRACT

In this research, ZnO nanorods - Au nanoparticles nanohybrids have been fabricated and employed to sensitive electrochemical strategy for the specific detection of the ovarian cancer antigen CA-125/MUC126. The microdevice was developed in our lab based on gold and silver electrodes sputtered on glass substrate. The ZnO nanorods arrays were grown on working electrode using assisted microwave hydrothermal synthesis than gold nanoparticles (Au NPs) were deposited by sputtering. The Au NPs onto ZnO nanorods surface provides a favorable platform for efficient loading of anti-CA-125 antibody via binding with cystamine and glutaraldehyde. The effective loading of the biological material (CA-125 antibody and antigen) on the matrix was observed by SEM images. The electrochemical immunosensor shows a sensitive response to ovarian cancer antigen recombinant human CA-125/MUC126 with detection of 2.5 ng/μL, 100 times lower than immunoblot system. Due to high specificity, reproducibility and noteworthy stability, the developed sensor will provide a sensitive, selective and convenient approach to be used to detect CA-125/MUC126.

Contents

1. Introduction

Recently, the development of ultra-sensitive biosensors has been studied because of it allows fast and specific detection of serious or deadly illness molecular markers whose early detection is of fundamental importance in successfully in treating of the disease [1].

Extensive research to achieve a simple, inexpensive and accurate device that employs biochemical molecular recognition properties as the basis of a selective analysis has opened new possibilities for using biosensors for patient diagnosis [2]. Among several types of biosensors, nanomaterials-based electrochemical immunosensors emerge as a promising technology due to features such as high sensitivity,

* Corresponding author.
E-mail address: talita.mazon@cti.gov.br (T. Mazon).

http://dx.doi.org/10.1016/j.msec.2017.02.031
0928-4931/

specificity, simplicity and inherent miniaturization, resulting in low cost and short time analysis [3–7]. Despite the advances in nanomaterials-based electrochemical immunosensors, some issues still need to be considered, like the design and engineering of biosensors and the amplification of signals [1–3].

To improve the amplification of faint sensing signals and the sensitivity of biosensors, a great variety of nanomaterials and nanostructures, including gold nanoparticles (AuNPs) and ZnO nanostructures, have been exploited, although little is known about the effectiveness of them [8–12].

The use of Au NPs assists on immobilization of biological entities due to their interesting physicochemical properties and possibility of modifying the surface by thiolated biomolecules [13–16]. Researchers have reported that immobilization of biomolecules on AuNPs improves the stability and aids preserving the activity of biomolecules [13–27]. Besides of this, the direct electron transfer between redox species and bulk electrode materials is facilitated by using Au NPs due to their conductor nature and enhances the electrochemical sensing [14].

On the other hand, ZnO nanostructures have been utilized as matrix in biosensors due to nice biocompatibility and biomimicry, large specific area, high chemical stability and high isoelectric point (IEP ~ 9.5) that make them favorable to immobilize and modify proteins [17–21]. Due to their semiconductor properties, ZnO nanostructures also provide an ideal channel for effective carrier transport during the redox process [22].

Recently, Perumal et al. [23] prepared hybrid gold nanostructures seeded into nanotextured zinc oxide nanoflowers (ZnO NFs) for biosensing applications. They reported that the specific interaction of Au NPs with DNA from pathogenic Leptospirosis causes strains via hybridization and mismatch. According to them, the distributed AuNPs on ZnO NFs can act as a single platform for multiple detection strategies. Nevertheless, the interaction of 1D ZnO nanostructures with a variety of biomolecules needs more study.

Although ZnO nanostructures have been studied as a biosensor matrix to detect enzymes related to a great number of illnesses, there are a few reports in the literature about biosensors based on ZnO nanostructures for detecting ovarian cancer [24–25]. The development of point-of-care biosensor systems to early detection of cancer may support in new means of treatment for tumors by improving patient care through real-time and remote health monitoring [26,27]. However, it is necessary to find requirements such as rapid label-free detection, miniaturized sensor size, low cost, and portability. Moreover, there are few efforts on integrating of the ZnO nanostructures with commercial detection systems for their real application in biosensor devices.

Among the various oncomarkers related to ovarian cancer, the mucin 16 (MUC16 or CA-125) is a blood-circulating antigen (Ag) that consists on a high molecular weight glycoprotein found on the surface of ovarian cancer cells [27–30]. Studies showed that 90% of women may test positive for CA-125 when they were diagnosed with the cancer [31].

So, the early sensitive detection of CA-125, as well as, the development of a high sensitivity, low cost immunosensor specific to CA-125 are important issues for early clinical diagnoses.

Ren et al. [31] proposed a sensitive electrochemical immunosensor based on ferro-cenecarboxylic acid (FA), HCl-doped polyaniline (H-PANI), chitosan hydrochloride (CS-HCl) and Ag@Co_3O_4 nanosheets for detection of CA-125. The electrochemical immunosensor was characterized by electrochemical impedance spectroscopy (EIS) using $[Fe(CN)_6]^{3-/4-}$ in solution as the redox probe and the limit of detection was 0.25 pg/mL [31]. Raghav [32] and collaborators reported a copper(II) oxide nanoflakes based impedimetric immunosensor for detection of cancer antigen 125 with a lower limit of detection (0.77 IU/mL). Nguyen and collaborators [33] developed a SERS immunosensor built-in microfluidic system based on Rhodamine-6G (R6G)-conjugated immunogolds with limit of detection of 15fM. Li et al. [34] developed an alternative electrochemiluminescence method to fabricate ultrasensitive sensor for detection of CA-125 based on dendrimer and magnetic nanoparticles with a detection limit of 0.032 μU/mL.

Despite the advantages of the above-mentioned sensors, the use of simpler and easier to be synthesized biosensor matrix, and low-cost technologies for detection are issues that need for improvements on developing point-of-care biosensors economically feasible.

In this work, we proposed to engineering a novel electrochemical immunosensor specific to CA-125 based on ZnO nanorods (NRs)-Au NPs nanohybrids immobilized with anti-CA-125 antibody. The effective loading of the biological material on the matrix was observed by SEM images. The sensitivity of the simpler and low-cost biosensor prepared here was 2.5 ng/μL, 100 times higher than the immunoblotting test.

2. Experimental section

2.1. Chemical

Zinc acetate dehydrate ($(CH_3CO_2)_2Zn\cdot 2H_2O$), zinc nitrate hexahydrate ($Zn(NO_3)_2\cdot 6H_2O$) and ethylene glycol were purchased from Synth. Citrate acid was purchased from Merck. Hexamine (HMTA) ($C_6H_{12}N_4$), potassium ferri/ferrocyanide $[Fe(CN)_6]^{3-/4-}$, dibasic sodium phosphate heptahydrate (Na_2HPO_4) and monobasic potassium phosphate (KH_2PO_4) were purchased from Sigma Aldrich. Anti-CA-125 antibody solution and recombinant human CA-125/MUC16 were purchased from Novus Biologicals and R&D Systems, respectively.

Phosphate buffered saline (PBS) was prepared by compounding solutions of NaH_2PO_4 (0.01 M) and Na_2HPO_4 (0.1 M) to pH 7.4 and 0.15 mol/L NaCl as support electrolyte for all electrochemistry measurements.

2.2. Synthesis of ZnO NRs-Au NPs nanohybrids

ZnO nanostructures have been synthesized by using a seeding layer of ZnO prepared by Pechini method followed by the assisted microwave hydrothermal synthesis, as discussed below.

2.2.1. Preparation of ZnO seeding layer

A solution of zinc citrate was prepared by Pechini method [35]. Zinc acetate dehydrate, $(CH_3CO_2)_2Zn\cdot 2H_2O$ was dissolved, under heat and stirring, in a solution of citric acid and ethylene glycol in the ratio 1:4:16, respectively. The solution was spin-coated onto a glass substrate. Glass substrate was coated with Au trails by RF sputtering (Denton Vacuum, model DV-502AP) prior to solution deposition. Subsequently, the precursor thin film was treated at 400 °C to remove organic materials and promote the formation of the ZnO crystalline phase.

2.2.2. Preparation of ZnO NRs-Au NPs nanohybrids

ZnO NRs were grown over the seed layer using assisted microwave hydrothermal synthesis. Zinc nitrate hexahydrate, $Zn(NO_3)_2\cdot 6H_2O$, 99.0%, and hexamethylenetetramine, HMTA - $C_6H_{12}N_4$, 99.0%, were mixed an equimolar aqueous solution. The reagents and the glass substrate were put in a Teflon cup and the hydrothermal process was carried out at 90 °C for 1 h. The substrates were then withdrawn from the solution followed by thorough washing with deionized water and then dried in air. Aiming to form ZnO NRs- Au NPs nanohybrids, the nanostructure obtained were sputter coated with Au using a Bal-Tec model SCD 050 by 2–5 s. After that, the nanohybrids were treated at 400 °C for 1 h. The nanohybrids were characterized by X-ray diffraction (XRD) by using the diffractometer XRD Rigaku 2000 with monochromatized graphite radiation, Scanning Electron Microscopy and energy dispersive X-ray spectroscopy (EDX) by using a JEOL – JSM 7500F.

2.3. Fabrication of ZnO NRs-Au NPs nanohybrids electrochemical immunosensor

The electrochemical immunosensor used here was developed in our group by using glass as a substrate having in its surface gold (Au) as working and counter electrodes and silver (Ag) as reference electrode, being configured each to be electrically isolated from the others. The metals were sputtered by using a sputtering Denton Vacuum, DV-502A model.

To the self-assembly process of the electrode, ZnO NRs-Au NPs nanohybrids were grown onto the working electrode, as described above. Subsequently, the modified electrode was coated with 20 μL of cystamine solution 20 mM, 20 μL of glutaraldehyde solution 2.5%, washed with deionized water and dried in air. Then, 10 μL of anti-CA-125 antibody solution diluted in PBS in the ratio 1:1000 was immobilized onto the surface of Zn NRs-Au nanohybrids based electrode. The anti-CA-125/MUC16 antibody used here was a CHO-derived, (NBP1-96619), MUC16 (Novus Biologicals). So, the functionalized electrode was washed with deionized water to remove the physically adsorbed anti-CA-125 and it was stored at 4 °C overnight. Finally, different concentration of the recombinant human CA-125/MUC16 was added to the bioelectrode and after that, the bioelectrode was immersed in PBS. The obtained immune sensor was stored in the refrigerator (4 °C) to retain its characteristics when not use.

Cyclic voltammetric (CV) measurements were carried out on a Potentiostat/Galvanostat (Metrohn-Autolab PGSTAT 128 N) in a 0.1 M PBS solution containing 5 mM potassium ferri/ferrocyanide $[Fe(CN)_6]^{3-/4-}$ as mediator and scan rate of 100 mV/s.

The detailed schematic for the preparation of the ZnO NRs-Au NPs nanohybrids based balustrade is shown in Fig. 1.

3. Results and discussion

The XRD spectra of the ZnO nanorods over glass substrate are shown in Fig. 2. It is possible to verify well-defined peaks corresponding to the hexagonal structure of ZnO with preferred (002) orientation, according to JCPDS 36-1451 [22,36]. A typical wurtzite ZnO structure has polar nature consisting of polar and non-polar faces [37,38]. The polar faces, (002) plane, show thermodynamic instability and to minimize the surface energy, it grows along the (002) plane faster than the other directions [37,38]. The (002) face of the crystal becomes either positively or negatively charged and this attracts ions of opposite charges (O^{2-} or Zn^{2+}) to it. After covered, the surface will attract ions with opposite charges to cover the surface next making possible the growth of ZnO nanorods [37,38].

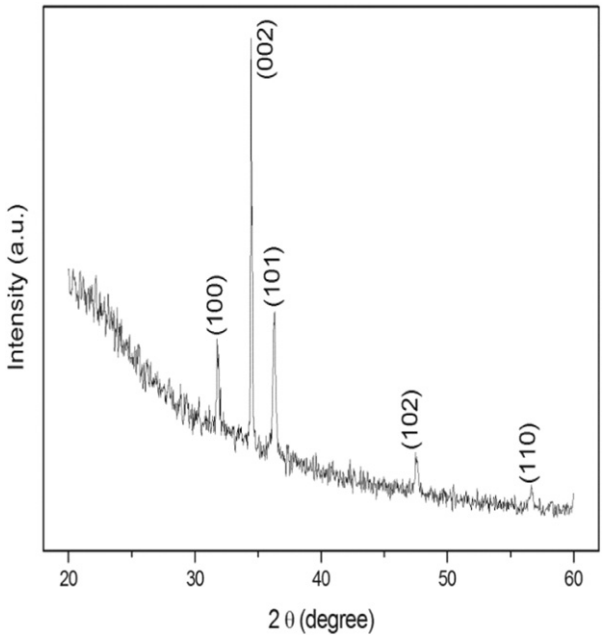

Fig. 2. XRD patterns of ZnO nanostructures grown on glass substrates by microwave assisted hydrothermal synthesis.

Fig. 3 shows the SEM images of nucleation layer (NL) deposited over working electrode, as well as, ZnO NRs and ZnO NRs-Au NPs

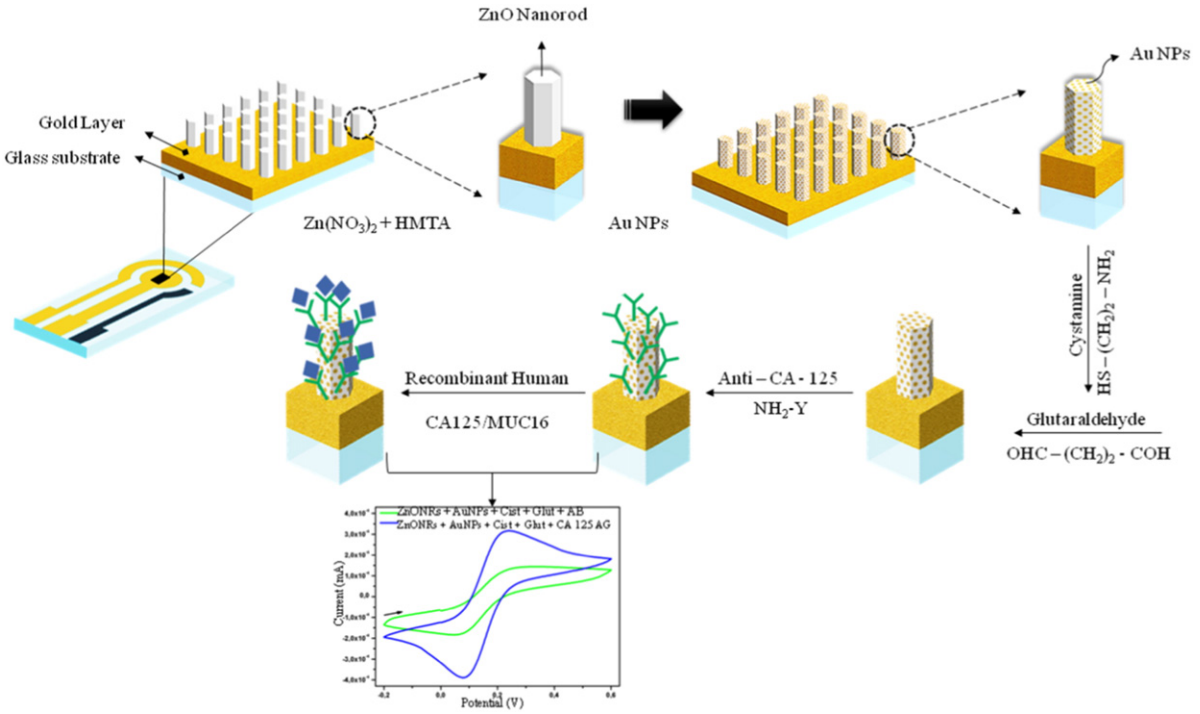

Fig. 1. Fabrication scheme of ZnO NRs-Au NPs nanohybrids biosensor for CA-125 detection.

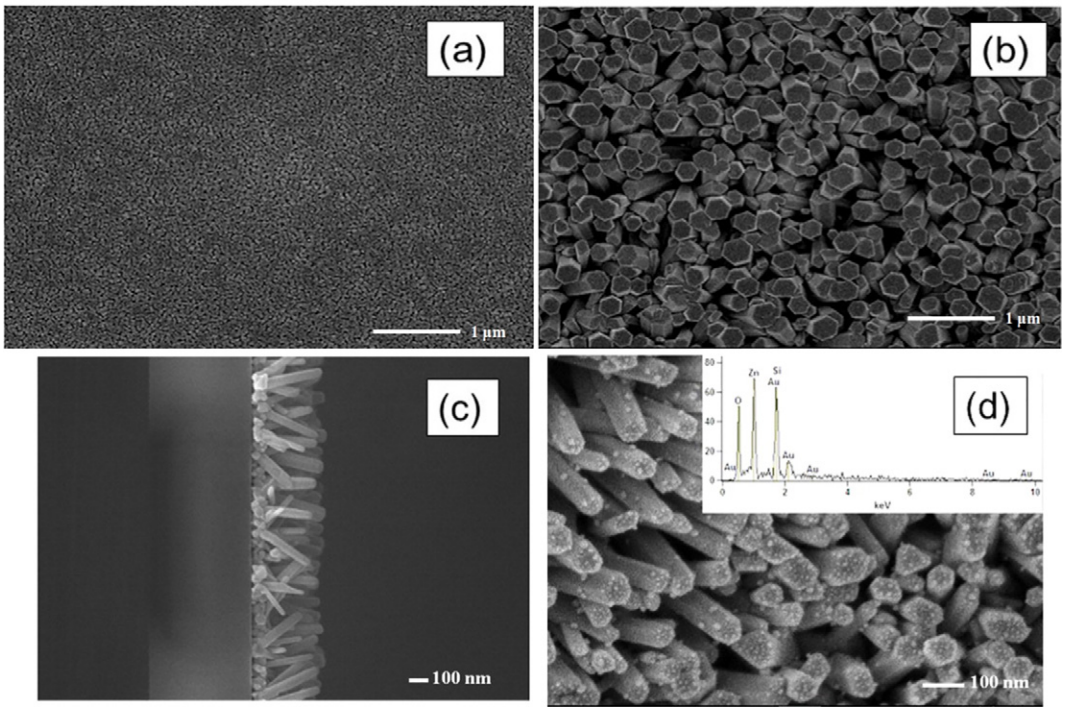

Fig. 3. SEM surface micrographs of nucleation layer (NL) (a); ZnO NRs top view (b); ZnO NRs cross section image (c); and ZnO NRs-Au NPs nanohybrids top view and EDS analysis inset.

nanohybrids obtained after synthesis and functionalization steps. It can be seen that nucleation layer is a homogeneous film with small grain size and porous microstructure (Fig. 3.a). These characteristics are fundamental for favoring the growth of perpendicular-aligned ZnO nanorods, as shown in Fig. 3.b and 3.c. The ZnO nanorods grown are dense and show hexagonal base with diameter around 70–80 nm and length around 400 nm. Fig. 3.d shows the image of the ZnO NRs after Au deposition and heating treatment at 400 °C. It can be seen a large number of Au nanoparticles over nanorods surface with good dispersion, uniform, spherical shape with diameter in the range 5 to 10 nm. Energy dispersive spectrometry (EDS) analysis, Fig. 3.d inset, revealed that the sample composition was Zn, O and Au, which proves the successful preparation of Au NPs functionalized ZnO nanorods. The simple methodology development here leads to excellent homogeneity of Au nanoparticles size and ZnO nanorods surface coverage with Au NPs compared with the chemical solution methodologies reported in the literature [39–43].

Besides of this, it is possible to notice (Fig. 3.d) that the multi-level architecture of Au NPs over ZnO NRs would provide a higher surface area for anti-CA-125 antibody immobilization compared to other competing methods, like planar graphene sheet or gold thin film deposited on graphene [44–45]. Considering that large surface area for high enzyme loading is a key point in the fabrication of bioelectrodes [22], the ZnO NRs-Au NPs nanohybrids based electrodes have been employed for the biosensor fabrication.

Figs. 4, 6 and 7 show the cyclic voltammograms (CV) obtained for the different electrodes in the potential window of −0.2 V to +0.6 V at the scan rate of 100 mV/s recorded in 0.1 M PBS solution containing 5 mM $[Fe(CN)_6]^{3-/4-}$ as the redox species. The cyclic voltammograms show well defined oxidation and reduction peaks in the presence of $[Fe(CN)_6]^{3-/4-}$ mediator which provides an electron communication path at a lower potential. All measurements were made in triplicate and the results obtained reveal the reproducibility of measurements and show the higher reliability of prepared bio-electrode for CA-125 detection.

The calibration curve of the bare sensor is shown in Fig.4.a. All the 16 curves showed the same electrochemical behavior proving excellent stability, reproducibility and reliability of the bare sensor developed here.

In order to study the behavior of the bare sensor without ZnO NRs-Au NPs matrix, the biological material was immobilized directly on the bare sensor. No change was observed in the magnitude of redox peak currents of the cyclic voltammogram in the presence or absence of the CA-125 antigen (CA-125 Ag) (Fig. 4.b). The reduction and oxidation peaks in the absence of the CA-125 Ag are located at 0.22 and 0.13, respectively. The cathodic current peak (I_{pc}) for the bare sensor with Ab is 1.27 mA. These values are similar to the obtained in the presence of 0.25 µg/µL CA-125 Ag (I_{pc} 1.32 mA). It indicates that the bare sensor doesn't work as an electrochemical immunosensor for itself.

On the other hand, the use of ZnO NRs-Au NPs nanohybrids as working electrode leads to changes in the magnitude of the cathodic current peaks (I_{pc}) in the presence or absence of CA-125 Ag (Fig. 4.b). The I_{pc} were 0.11 mA and 0.38 mA in absence and presence of 0.25 µg/µL CA-125 Ag, respectively. The variation of change in the I_{pc} indicates that the electron transference process increases in the presence of the antigen. This suggests firstly, the immobilization of the antibody over the surface of ZnO NRs-Au NPs nanohybrids and secondly, the linkage between antibody (Ab) and antigen (Ag). As well known, thiols coordinate very strongly onto a variety of metals, e.g., gold due to deprotonation of thiol groups upon adsorption [44]. In this work, the cystamine (Cyst), an organic amine disulfide, was used to modify the Au NPs surface by introducing amine groups when it is adsorbed upon Au NPs surface via thiol group. These amine groups are covalently bound with glutaraldehyde (Glut) [24]. The Glut reacts with CA-125 Ab amine groups giving a specific link to capture the CA-125 Ag and ensure the antigen-antibody specificity phenomenon. The sensing mechanism of CA-125 Ag through the bioelectrodes is shown in Fig. 1.

The surface of the ZnO NRs-Au NPs hybrids materials was analyzed by SEM after antibody immobilization and linkage with the antigen (Fig. 5). A protein thick layer deposited was observed showing very high antibody loading due not only to very high surface area provided by the grown ZnO nanostructures functionalized with Au NPs but also to the presence of thiols group from Cyst, that coordinate with Au NPs

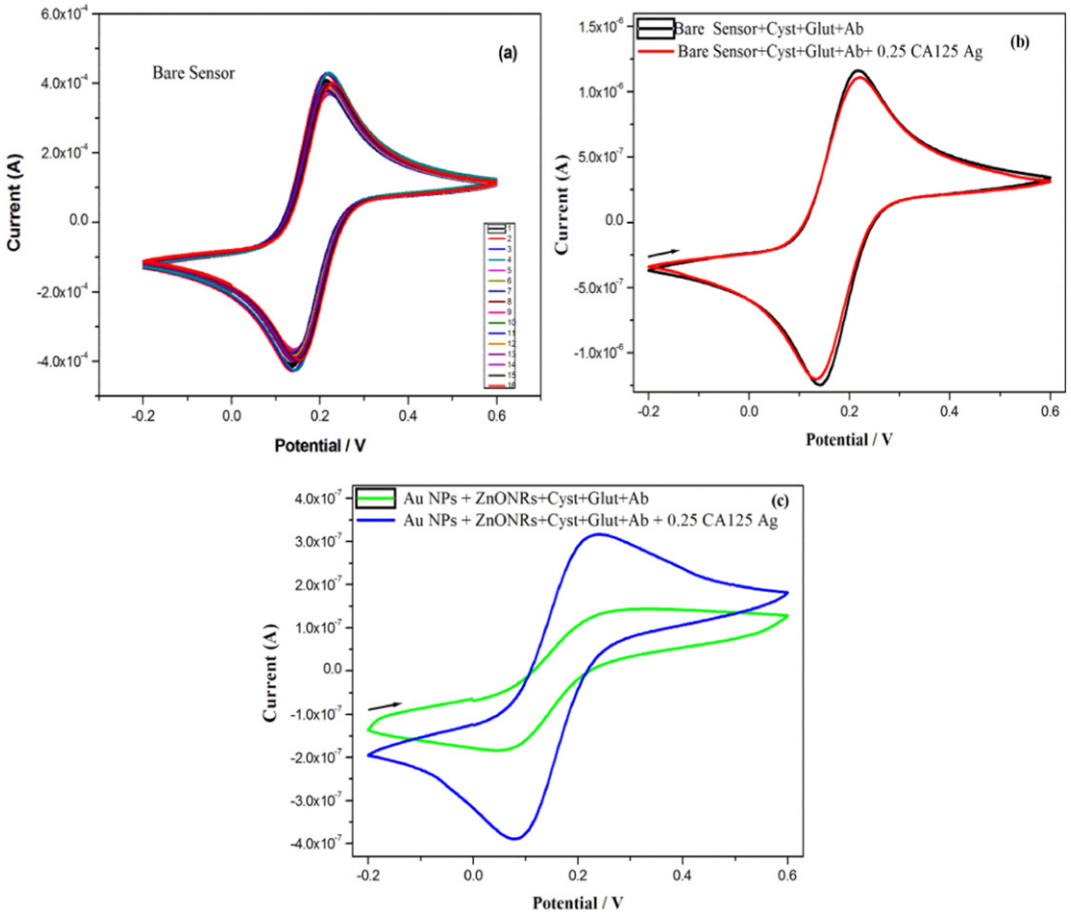

Fig. 4. Cyclic voltammograms of (a) 16 calibration curves of the bare sensor; (b) bare sensor immobilized with cystamine (Cyst), glutaraldehyde (Glut) and anti-CA-125 antibody (Ab) in the absence and presence of 0.25 μg/μL CA-125 antigen (0.25 CA-125 Ag) and (c) ZnO NRs-Au NPs hybrids bioelectrodes immobilized with Cyst, Glut and Ab in the absence and presence of 0.25 CA-125 Ag. The curves were recorded in 0.1 M PBS solution containing 5 mM $[Fe(CN)_6]^{3-/4-}$ as a redox mediator.

resulting in complete coverage of the sample surface by the immobilized antibody. It is also possible to observe that the anti-CA-125 antibody shows morphology like Y-shaped molecules with two arms (Fig. 5.a) that change to ribbons interleaved with loops (Fig. 5.b) after binding with the antigen. The size of the structures is around 20 nm, very close to protein size reported in the literature. These SEM images are very similar with the pictures of the basic antibody and antigen structures reported by Greene et al. [46]. As far as the authors know it is the first time that antibody and antigen structures are reported by using SEM images.

The electrochemical sensing response of the ZnO NRs-Au NPs nanohybrids immobilized with cystamine (Cyst), glutaraldehyde (Glut) and anti-CA-125 antibody (Ab) bioelectrodes as a function of the recombinant human CA-125/MUC16 antigen concentration (Ag concentration, x = 0.50 μg/μL, 0.25 μg/μL; 25 ng/μL and 2.5 ng/μL) is shown in Fig. 6.a and Fig. 6.b. The well-defined CV curves are obtained for the bioelectrode prepared at all measured concentrations of Ag. The magnitude of the cathodic current peak was found to increase with Ag concentration. It can be seen in Fig. 6.a that I_{pc} increase further to 0.38 mA for 0.25 μg/μL and 0.61 mA for 0.50 μg/μL. The same behavior was observed at lower Ag concentrations, where the I_{pc} increases further to 0.42 mA for 2.5 ng/μL and 0.46 mA for 25 ng/μL.

The increasing of the I_{pc} as a function of increasing the Ag concentration suggests that the binding of antigen and antibody help in the charge

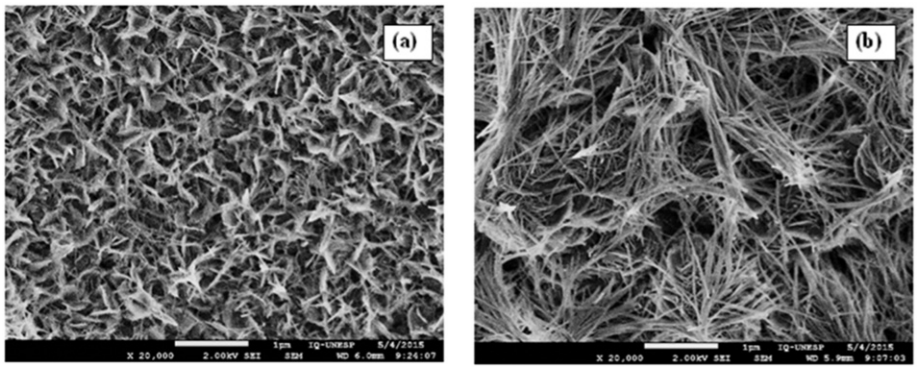

Fig. 5. SEM images of immunosensor based on ZnO NRs-Au NPs nanohybrids immobilized with: (a) Cyst, Glut and Ab; and (b) Cyst, Glut, Ab and 0.25 μg/μL CA-125 Ag.

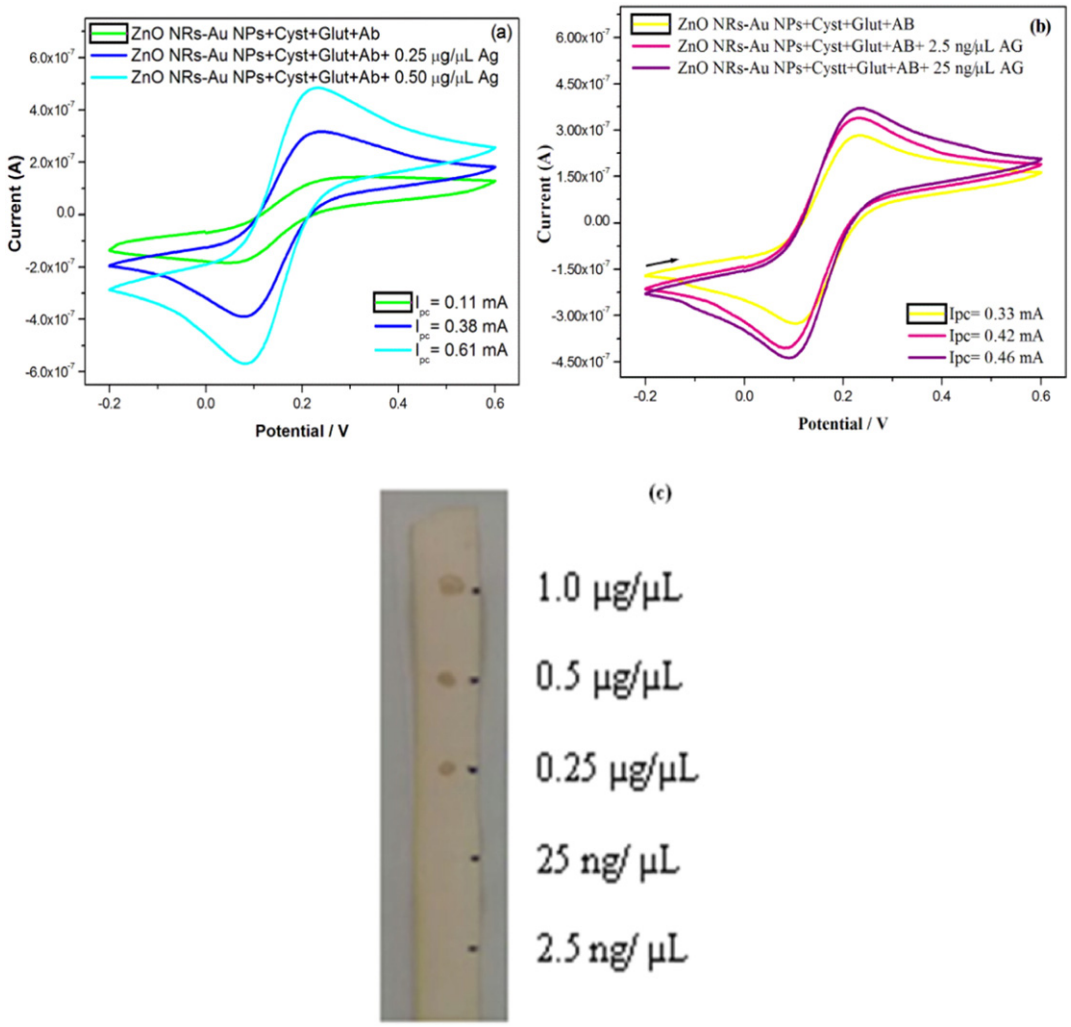

Fig. 6. Cyclic voltammograms of (a) ZnO NRs-Au NPs hybrids bioelectrodes immobilized with Cyst, Glut, Ab and 0.25 or 0.50 μg/μL CA-125 Ag; (b) ZnO NRs-Au NPs hybrids immobilized with Cyst, Glut, Ab and 2.5 or 25 ng/μL CA-125 Ag. The curves were recorded in 0.1 M PBS solution containing 5 mM $[Fe(CN)_6]^{3-/4-}$ as a redox mediator. (c) nitrocellulose membrane used in the immunobloting test for quantitative determination of CA-125 Ag and semi-quantitative of the anti-CA-125 antibody.

transference process. As the Ag concentration increases, biochemical reactions take place resulting in a release of more number of electrons. So, an increase in CV peak oxidation current is observed.

The Fig. 6.c shows the nitrocellulose membrane after immunoblotting test. It is possible to see that the immunoblotting showed detection limit of 0.25 μg/μL for the CA-125 Ag.

The CV curves obtained just for ZnO NRs-Au NPs nanohybrids and ZnO NRs-Au NPs nanohybrids immobilized with Cyst and Glut samples (Fig. 7) in the absence of Ag can also support the idea of occurrence of biological reactions between Ag and Ab. On the contrary of shown in Fig. 6, the I_{pc} decreases as the nanostructures and biological material are added (Fig. 7). In this case, the transfer of electrons between the electrode and the electrolyte is obstructed due to the insulating nature of the immobilized biological material onto the ZnO NRs-Au NPs surface.

The possible sensing mechanism of the recombinant human CA-125/MUC16 antigen using the prepared bioelectrodes is shown in Fig. 1. The main role of ZnO NRs-Au NPs nanohybrids is to provide a favorable environment for the immobilization of anti-CA-125 antibody. Firstly, nanohybrids are functionalized with cystamine to get amino groups on the surface (Eq. (1)). These amino groups bind with glutaraldehyde for providing carbonyl groups on the surface (Eq. (2)). The carbonyl groups are easily bound with the amino groups of the anti-CA-125

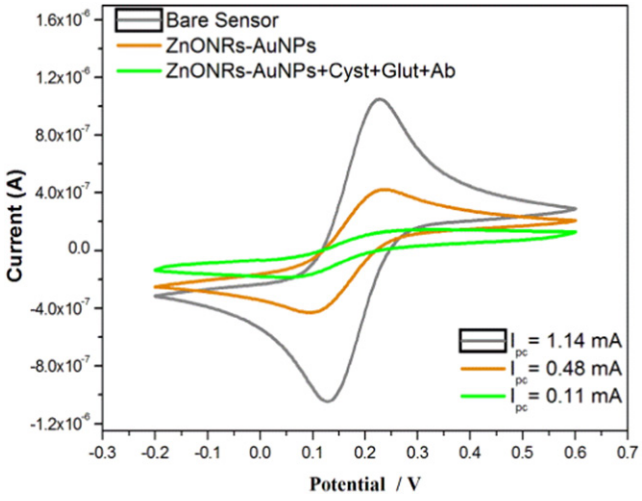

Fig. 7. Cyclic voltammograms of the bare sensor, ZnO NRs-Au NPs hybrids and ZnO NRs-Au NPs hybrids immobilized with cystamine (Cyst), glutaraldehyde (Glut) and anti-CA-125 antibody (Ab). The curves were recorded in 0.1 M PBS solution containing 5 mM $[Fe(CN)_6]^{3-/4-}$ as a redox mediator.

antibody (NH_2-Y) (Eq. (3)).

$$\mathrm{ZnO\ NRs-Au} \xrightarrow{\mathrm{HS-(CH2)2-NH2}} \mathrm{ZnO\ NRs-Au-S-(CH_2)_2-NH_2} \quad (1)$$

$$\mathrm{ZnO\ NRs-Au-S-(CH_2)_2-NH_2} \xrightarrow{\mathrm{OHC-(CH2)2-CHO}} \mathrm{ZnO\ NRs-Au-S-(CH_2)_2-N=CH-(CH_2)_2-CHO} \quad (2)$$

$$\mathrm{ZnO\ NRs-Au-S-(CH_2)_2-N=CH-(CH_2)_2CHO} \xrightarrow{\mathrm{NH2-Y}} \mathrm{ZnO\ NRs-Au-S-(CH_2)_2-N=CH-(CH_2)_2-CH=N-Y} \quad (3)$$

As well known, the antibody is a Y-shaped molecule consisting of two arms and a stem connected by disulfide links [45]. The disulfide linkers allow a flexible movement in the antibody bound on the ZnO NRs-Au NPs nanohybrids surface [45]. The arms containing amino groups will bind with functionalized nanohybrids and a variable region (denominated Y in Eq. (3)) will work as an antigen binding site. In the presence of CA-125 antigen, the antigen binding domains loops mediate antigen specificity and binding [45]. Probably, in our case, after binding the CA-125 antigen loss electrons which assist in the reduction of $[Fe(CN)_6]^{3-}$ ions into $[Fe(CN)_6]^{4-}$ ions present in the solution. The $[Fe(CN)_6]^{4-}$ ions are again oxidized to $[Fe(CN)_6]^{3-}$ ions during forward CV scan and the transfer of electrons to the Au bottom electrode occurs via ZnO NRs-Au NPs nanohybrids matrix.

The observed results obviously indicate the importance of ZnO NRs-Au NPs nanohybrids as a matrix biosensor. It was possible to detect 2.5 ng/μL of CA-125 antigen, 100 times lower than immunoblot system. This higher value of sensitivity is a result of high adsorption, effective antibody loading and possible fast electron communication characteristics of the ZnO nanostructures and Au nanoparticles, as also observed for enzymatic glucose and urea detection [2,10,22].

The biosensing response measurements were repeated in triplicate and the bioelectrode samples were prepared under identical processing conditions. Similar results were obtained within experimental error implying that the ZnO NRs-Au NPs nanohybrids based bioelectrode matrix provides stable and reproducible results.

4. Conclusions

ZnO NRs-Au NPs nanohybrids based matrix has been synthesized by hydrothermal and sputtering methods and has been exploited for detection of CA-125, an ovarian cancer marker. ZnO NRs-Au NPs nanohybrids matrix provides a favorable platform for efficient loading of anti-CA-125 antibody via binding with cystamine (Cyst) and glutaraldehyde (Glut). The immunosensor shows a relatively low detection limit of 2.5 ng/μL, good stability and reproducibility. The high sensitivity highlights the importance of ZnO NRs-Au NPs nanohybrids matrix which provides an appropriate surface for the immobilized anti-CA-125 antibody preserving its active sites. Thus, the fabricated immunosensor may have a promising application prospect in clinical diagnosis.

Acknowledgements

The authors would like to be thankful to CNPq (455193/2013) and the Center for Research and Development of Functional Materials CEPID - FAPESP (2013/07296-2) Brazilian Agencies by the financial support and the LME/LNNano - Brazilian Nanotechnology National Laboratory/CNPEM/MCTI by the support in SEM images.

References

[1] L. Zhang, Y. He, H. Wang, Y. Yuan, R. Yuan, Y. Chai, A self-enhanced electrochemiluminescence immunosensor based on L−Lys−Ru (dcbpy)$_3^{2+}$ functionalized porous six arrises column nanorods for detection of CA 15-3, Biosens. Bioelectron. 74 (2015) 924–930.
[2] Q. Ma, K. Nakazato, Low-temperature fabrication of ZnO nanorods/ferrocenyl-alkanethiol bilayer electrode and its application for enzymatic glucose detection, Biosens. Bioelectron. 51 (2014) 362–365.
[3] R. Rahmanian, S.A. Mozaffari, Abedi, Disposable urea biosensor based on nanoporous ZnO film fabricated from omissible polymeric substrate, Mater. Sci. Eng. C 57 (2015) 387–396.
[4] D. Liu, L. Wang, S. Ma, Z. Jiang, B. Yang, X. Han, S. Liu, A novel electrochemiluminescent immunosensor based on CdS-coated ZnO nanorod arrays for HepG2 cell detection, Nanoscale 7 (2015) 3627–3633.
[5] F. Liu, Y. Zang, J. Yu, S. Wang, S. Ge, X. Song, Application of ZnO/graphene and S6 aptamers for sensitive photoelectrochemical detection of SK-BR-3 breast câncer cells based on a disposable índium tin oxide device, Biosens. Bioelectron. 51 (2014) 413–420.
[6] S.K. Arya, S. Saha, J.E. Ramirez-Vick, V. Gupta, S. Bhansali, S.P. Singh, Recent advances in ZnO nanostrutures and thin films for biosensor application: review, Anal. Chim. Acta 737 (2012) 1–21.
[7] M.F. Frasco, N. Chaniotakis, Semiconductor quantum dots in chemical sensors and biosensors, Sensors 9 (2009) 7266–7286.
[8] D. Zhang, Y. Zhang, C. Yang, C. Ge, Y. Wang, H. Wang, H. Liu, Nanotechnology 26 (2015) 335,502 (7 pp.).
[9] Y.H. Liang, C.C. Chang, C.C. Chen, Y.C. Su, C.W. Lin, Development of na Au/ZnO thin film surface plasmon resonance-based biosensor immunoassay for the detection of carbohydrate antigen 15-3 in human saliva, Clin. Biochem. 45 (2012) 1689–1693.
[10] L. Fang, B. Liu, L. Liu, Y. Li, K. Huang, Q. Zhang, Direct electrochemistry of glucose oxidase immobilized on Au nanoparticles-functionalized 3D hierarchically ZnO nanostructures and its application to bioelectrochemical glucose sensor, Sensors Actuators B Chem. 222 (2016) 1096–1102.
[11] Y.T. Wang, L. Yu, J. Wang, L. Lou, W.J. Du, Z.Q. Zhu, H. Peng, J.Z. Zhu, A novel L-lactate sensor based on enzyme electrode modified with ZnO nanoparticles and multiwall carbon nanotubes, J. Electroanal. Chem. 661 (2011) 8–12.
[12] M. Das, G. Sumana, R. Nagarajan, B.D. Malhotra, Application of nanostructured ZnO films for electrochemical DNA biosensor, Thin Solid Films 519 (2010) 1196–1201.
[13] Y. Xin, X.F. Bing, L.H. Wei, W. Feng, C.D. Zhao, W.Z. Yang, A novel H_2O_2 biosensor based on Fe_3O_4-Au magnetic nanoparticles coated horseradish peroxidase and graphene sheets – nafion film modified screen-printed carbon electrode, Electrochim. Acta 109 (2013) 750–755.
[14] T. Dodevska, E. Horozova, N. Dimcheva, Electrochemical behavior of ascorbate oxidase immobilized on graphite electrode modified with Au-nanoparticles, Mater. Sci. Eng. B 178 (2013) 1497–1502.
[15] V.K. Upadhyayula, Functionalized gold nanoparticle supported sensory mechanisms applied in detection of chemical and biological threat agents: a review, Anal. Chim. Acta 715 (2012) 1–18.
[16] S.W. Ryu, C.H. Kim, J.W. Han, C.J. Kim, C. Jung, H.G. Park, Y.K. Choi, Gold nanoparticle embedded silicone nanowire biosensor for applications of label-free DNA detection, Biosens. Bioelectron. 25 (2010) 2182–2185.
[17] M. Zhao, J. Huang, Y. Zhou, Q. Chen, X. Pan, H. He, Z. Ye, A single mesoporous ZnO/chitosan hybrid nanostructure for a novel free nanoprobe type biosensor, Biosens. Bioelectron. 43 (2013) 226–230.
[18] Z.H. Dai, G. Shao, J. Hong, J. Bao, J. Shen, Immobilization and direct electrochemistry of glucose oxidase on a tetragonal pyramid-shaped porous ZnO nanostructure for a glucose biosensor, Biosens. Bioelectron. 24 (2009) 1286–1291.
[19] S. Saha, V. Gupta, K. Sreenivas, H.H. Tan, C. Jagadish, Third generation biosensing matrix based on Fe-implanted ZnO thin film, Appl. Phys. Lett. 97 (2010) 133704-1–133704-3.
[20] T. Kong, Y. Chen, Y. Ye, K. Zhang, Z. Wang, X. Wang, An amperometric glucose biosensor based on the immobilization of glucose oxidase on the ZnO nanotubes, Sensors Actuators B Chem. 138 (2009) 344–350.
[21] S.G. Ansari, R. Wahab, Z.A. Ansari, Y.S. Kim, G. Khang, A. Al-Hajry, H.S. Shin, Effect of nanostructure on the urea sensing properties of sol–gel synthesized ZnO, Sensors Actuators B Chem. 137 (2009) 566–573.
[22] M. Tak, V. Gupta, M. Tomar, A highly efficient urea detection using flower-like zinc oxide nanostructures, Mater. Sci. Eng. C 57 (2015) 38–48.
[23] V. Perumal, U. Hashim, S.C.B. Gopinath, R. Haarindraprasad, K.L. Foo, S.R. Balakrishnan, P. Poopalan, Spotted nanoflowers': gold-seeded zinc oxide nanohybrid for selective bio-capture, Nat. Sci. Rep. 5 (2015), 12231. http://dx.doi.org/10.1038/srep12231.
[24] J. Wang, Electrochemical biosensors: towards point-of-care cancer diagnostics, Biosens. Bioelectron. 21 (2006) 1887–1892.
[25] A. Ravalli, G.P. Santos, M. Ferroni, G. Faglia, H. Yamanaka, G. Marazza, New label free CA125 detection based on gold nanostructured screen-printed electrode, Sensors Actuators B Chem. 179 (2013) 194–200.
[26] F. Leung, E.P. Diamandis, V. Kulasingam, Chapter two – ovarian cancer biomarkers: current state and future implications from high-throughput technologies, Adv. Clin. Chem. 66 (2014) 25–77.
[27] M. Johari-Ahar, M.R. Rashidi, J. Barar, M. Aghaie, D. Mohammadnejad, A. Ramazani, P. Karami, G. Coukos, Y. Omidi, An ultra-sensitive impedimetric immunosensor for detection of the serum oncomarker CA-125 in ovarian cancer patients, Nanoscale 7 (2015) 3768–3779.
[28] S. Sarojini, A. Tamir, H. Lim, S. Li, S. Zhang, A. Goy, A. Pecora, K.S. Suh, Early detection biomarkers for ovarian cancer, J. Oncol. 15 (2012), 709049. http://dx.doi.org/10.1155/2012/709049.
[29] D.L. Meany, L.J. Sokoll, D.W. Chan, Early detection of cancer: immunoassays for plasma tumor markers, Expert Opin Med. Diagn. 3 (2009) 597–605.

[30] R.C. Bast, Status of tumor markers in ovarian cancer screening, J. Clin. Oncol. 21 (2003) 200–205.
[31] X. Ren, H. Wang, D. Wu, D. Fan, Y. Zhang, B. Du, Q. Wei, Ultrasensitive immunoassay for CA125 detection using acid site compound as signal and enhancer, Talanta 144 (2015) 535–541.
[32] R. Raghav, S. Srivastava, Copper(II) oxide nanoflakes based impedimetric immunosensor for label free determination of cancer antigen-125, Sens. Lett. 14 (n. 1) (2016) 97–101 (5).
[33] A.H. Nguyen, J. Lee, H.I. Choi, H.S. Kwak, S.J. Sim, Fabrication of plasmon length-based surface enhanced Raman scattering for multiplex detection on microfluidic device, Biosens. Bioelectron. 70 (2015) 358–365.
[34] J. Li, Q. Xu, C. Fu, Y. Zhang, A dramatically enhanced electrochemiluminescence assay for CA125 based on dendrimer multiply labeled luminol on Fe3O4 nanoparticles, Sensors Actuators B Chem. 185 (2013) 146–153.
[35] Sprague Electric Company (Massachussets). M. P. Pechini and N. Adams. Method of preparing lead and alcaline earth titanates and niobates and coating method using the same to form a capacitor. US 3330697, July 11 1967.
[36] A. Vasudev, A. Kaushik, S. Bhansali, Electrochemical immunosensor for label free epidermal growth fator receptor (EGFR) detection, Biosens. Bioelectron. 39 (2013) 300–305.
[37] P.K. Samanta, S.K. Patra, P.R. Chaudhuri, Violet emission from flower-like bundle of ZnO nanosheets, Phys. E. 41 (2009) 664–667.
[38] Q. Li, V. Kumar, Y. Li, H. Zhang, T.J. Marks, R.P.H. Chang, Fabrication of ZnO nanorods and nanotubes in aqueous solutions, Chem. Mater. 17 (2005) 1001–1006.
[39] Y.C. Liang, W.K. Liao, X.S. Deng, Synthesis and substantially enhanced gas sensing sensitivity of homogeneously nanoscale Pd- and Au-particle decorated ZnO nano-structures, J. Alloys Compd. 599 (2014) 87–92.
[40] J. Guo, J. Zhang, M. Zhu, D. Ju, H. Xu, B. Cao, High-performance gas sensor based on ZnO nanowires functionalized by Au nanoparticles Sens, Actuators B 199 (2014) 339–345.
[41] F. Tian, Y. Liu, K. Guo, Au nanoparticle modified flower-like ZnO structures with their enhanced properties for gas sensing, Mater. Sci. Semicond. Process. 21 (2014) 140–145.
[42] J. Hu, F. Gao, S. Sang, P. Li, X. Deng, W. Zhang, Y. Chen, K. Lian, Optimization of Pd contente in ZnO microstructures for high-performance gas detection, J. Mater. Sci. 2015 (1935–1942) 50.
[43] X. San, G. Wang, B. Liang, Y. Song, S. Gao, J. Zhang, F. Meng, Catalyst-free growth of one-dimensional ZnO nanostructures on SiO_2 substrate and in situ investigation of their H_2 sensing properties, J. Alloys Compd. 622 (2015) 73–78.
[44] M. Pumera, Graphene in biosensing, Mater. Today 14 (7,8) (2011) 308–315.
[45] H.J. Yoon, T.H. Kim, Z. Zhang, E. Azizi, T.M. Pham, C. Paoletti, J. Lin, N. Rammnath, M.S. Wicha, D.F. Hayes, D.M. Simeone, S. Nagrath, Sensitive capture of circulating tumour cells by functionalized graphene oxide nanosheets, Nat. Nanotechnol. 8 (2013) 735–741.
[46] Th. Wink, S.J. van Zuilen, A. Bult, W.P. van Benneko, Self-assembled monolayers for biosensors, Analyst 122 (1997) 43R–50R.